HAIT Journal of Science and Engineering B, Volume 2, Issues 3-4, pp. 558-570

Analysis of current-controlled inductors by new SPICE behavioral model

Evgeny Rozanov and Sam Ben-Yaakov*

Power Electronics Laboratory, Department of Electrical and Computer Engineering, Ben-Gurion University of the Negev, Beer-Sheva 84105, Israel
**Corresponding author: sby@ee.bgu.ac.il*

Received 1 March 2005, accepted 17 August 2005

Abstract

A new SPICE-compatible behavioral model for an arbitrary nonlinear magnetic circuit was developed and verified experimentally. The proposed model was used to analyze a current controlled magnetic inductor behavior. The nonlinearity of the ferromagnetic medium was reproduced by applying the core manufacturer data. Close agreement was obtained between the simulation and experimental results.

1 Introduction

Current-controlled inductors are important building blocks of various power-electronic systems [1,2]. A current-controlled inductor (CCI) is based on the modulation (control) of the permeability of its ferromagnetic core by a bias magnetic field produced by an auxiliary (secondary) coil. SPICE compatible model of such nonlinear devices could be an important tool in the analysis, design, and optimization of such systems. However, simulation by PSPICE, or any other modern electronic circuit simulator of electronic circuits that include controlled magnetic devices, is a nontrivial task. This is because PSPICE libraries do not offer built-in models for simulating complex magnetic elements beyond a simple inductor or transformer. One possibility to overcome this obstacle is to represent such devices by PSPICE compatible equivalent electric models.

The objective of the present study was to analyze a current-controlled inductor by applying a new PSPICE compatible model in which the magnetic core properties are described by analytical expressions that are based on readily available manufacturers' data.

2 The current-controlled inductor

The current-controlled inductor analyzed in this study is built around a double 'E' core structure (Fig. 1) [1]. The basic idea of this device is to control the main (center-arm-wound) inductor by altering the outer arms permeances. For this purpose, two identical windings are placed on the outer arms of the core. These windings are serially connected in opposite polarity to form the bias winding that carries the bias current I_{bias}. The serial connection of the two outer arm windings should cancel out the voltage induced on each of them. This is because the induced voltages on the

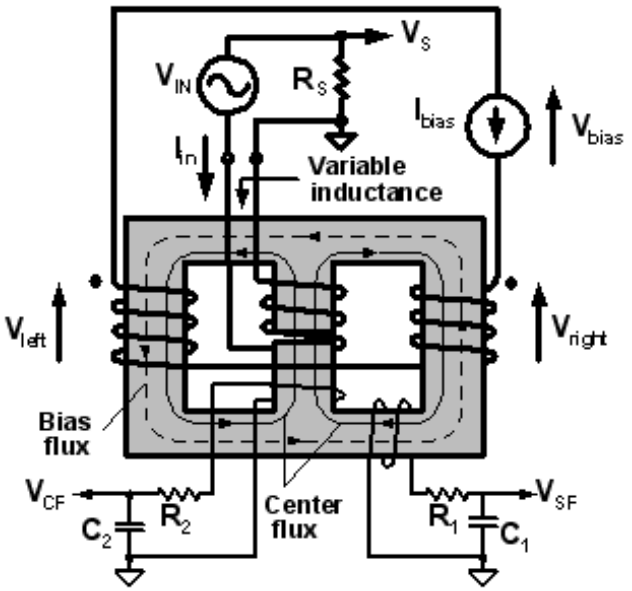

Figure 1: The current-controlled inductor [1] with measurements setup. The sense windings with RC integrator circuits are used for flux density B measurements. The voltage V_S on sense resistor R_S is proportional to the center arm magnetic field strength H.

windings have opposite polarities and, under the assumption of symmetry, should cancel each other. However, a closer examination of the problem shows the presence of a parasitic, non linear, coupling between the input voltage V_{in} and the bias windings voltage V_{bias}.

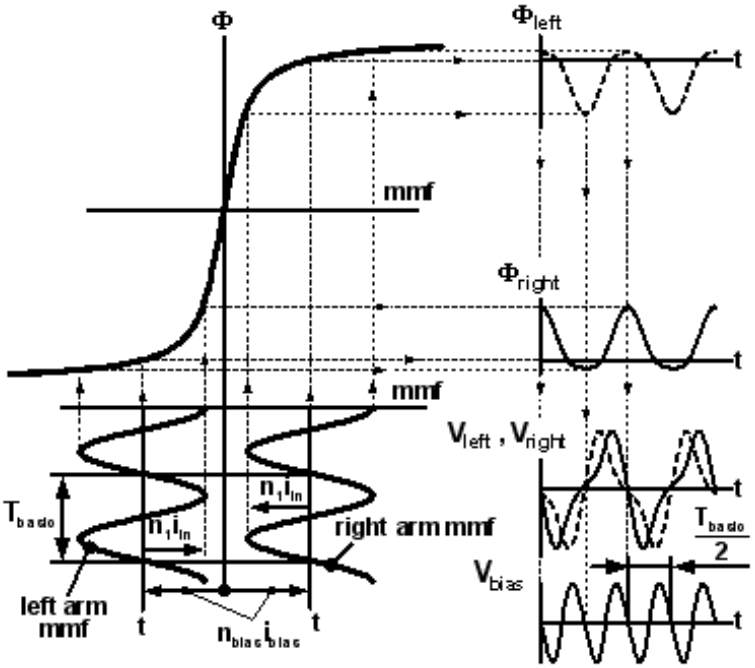

Figure 2: The basic frequency current I_{in} through center-arm-wound-inductor results in the double frequency voltage V_{bias} on outer arm windings.

The reason for a mutual coupling between the main inductor and the serially connected bias windings is the non-linearity of the magnetic material. This will be discussed by assuming a constant bias current I_{bias}. The bias current will produce a constant mmf ($I_{bias} \cdot n_{bias}$) in the outer arms that will bring these sections into the non-linear region of the B-H curve (Fig. 2). These mmf offsets are in opposite directions with respect to the mmf's originating from the central arm ($I_{in} \cdot n_1$). That is, at any given instance, the mmf induced by the arm will increase the permeance of one arm and reduce the permeance of the second one. Because of this non-symmetry in the permeances, the rate of change of the fluxes $\partial\Phi_{right}/\partial t$ and $\partial\Phi_{left}/\partial t$ will differ. That is, the instantaneous voltages induced on the right- and left-arm

windings V_{right}, V_{left} (Figs. 1 and 2) will be unequal and consequently, the difference $V_{bias} = V_{right} - V_{left}$ of the serially connected bias windings will be non zero. As can be observed by examining Fig. 2, the frequency of this voltage is double the frequency of the input current I_{in} (or input voltage V_{in}). The amplitude of the voltage V_{bias} depends on the amplitude of input voltage V_{in}, the value of bias current I_{bias}, the non-linear properties of magnetic material, and the number of turns n_1, n_{bias}. Since analytical estimation of these non-linear phenomena is extremely complicated, a PSPICE compatible model of the device could be extremely useful.

3 SPICE-compatible magnetic model

The proposed solution to the modeling of complex magnetic structures follows the concept of the gyrator-capacitor-model (GCM) [3,4]. It suggests employing a capacitor for emulation the magnetic energy storage element. The magnetic energy E_{mf} stored by any branch of magnetic circuit, can be expressed in terms of the flux Φ and the permeance P:

$$E_{mf} = \frac{\Phi^2}{2\,P}. \tag{1}$$

On the other hand, the storage of electric field energy E_{ef} of the capacitor can be expressed in terms of the electric charge Q and capacitance C:

$$E_{ef} = \frac{Q^2}{2\,C}. \tag{2}$$

The analogy between electrical and magnetic parameters in (1) and (2) is evident. The rest of equivalency can be found from the set of the following well-known equations:

$$P = \frac{\Phi}{mmf} = \frac{\int \frac{\partial \Phi}{\partial t} dt}{mmf} \tag{3}$$

where $mmf = H \cdot l_e$ is the magnetomotive force, H is the magnetic field strength, and l_e is effective magnetic branch length.

The analogous electrical equation is:

$$C = \frac{Q}{V_C} = \frac{\int \frac{dQ}{dt}\, dt}{V_C} \tag{4}$$

where Q and V_C are, respectively, the charge of and voltage at the capacitor C.

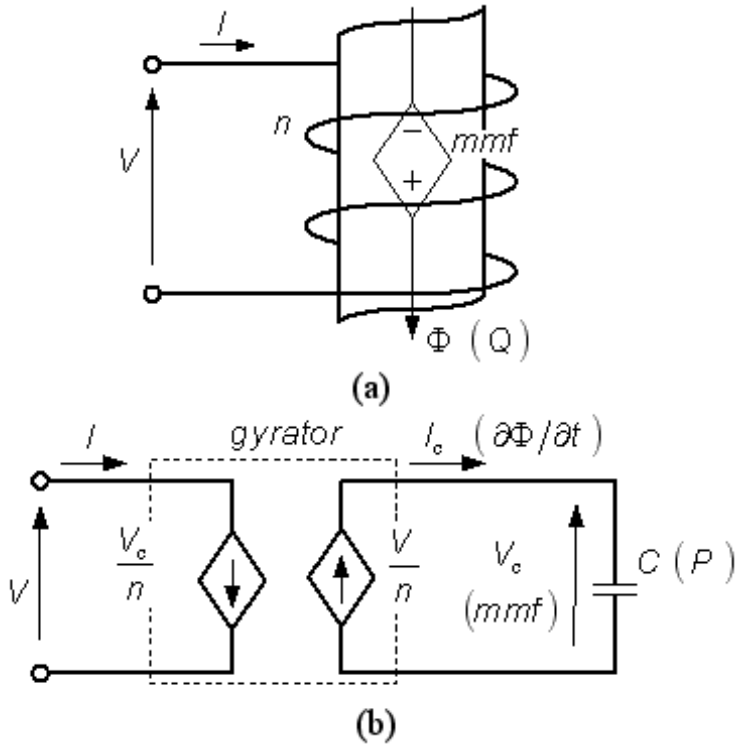

Figure 3: A simple magnetic branch (a) and its equivalent gyrator-capacitor model (b).

To emulate electromagnetic link between the voltage, current, and magnetic field of the windings, the model must reflect the Faraday and Ampere laws:

$$\frac{\partial \Phi}{\partial t} = -\frac{V}{n}, \tag{5}$$

$$I = \frac{mmf}{n}. \tag{6}$$

Based on the above, the electrical equivalent circuit of a magnetic circuit can be developed as follows. From (1),(2):

$$C \equiv P, \tag{7}$$

$$Q \equiv \Phi. \tag{8}$$

From (3)

$$mmf = P \cdot \Phi, \tag{9}$$

$$V_C = C \cdot Q \tag{10}$$

and hence

$$V_C \equiv mmf. \tag{11}$$

Defining

$$I_C \equiv \frac{\partial \Phi}{\partial t}, \tag{12}$$

one can translate (5) into

$$I_C \equiv -\frac{V}{n} \tag{13}$$

and from (6) and (11)

$$I \equiv \frac{V_C}{n}. \tag{14}$$

Consequently, equations (7), (13), (14) can be used to emulate the magnetic circuit of Fig. 3a by a gyrator that is loaded by a capacitor of value P (Fig. 3b).

4 Modeling of non-linear magnetic properties

A prerequisite for simulating a magnetic circuit that applies practical magnetic cores, is the ability to take into account the nonlinearity of the permeances.

From (3):

$$P_{e\,i} = \frac{\Phi_i}{mmf_i} = \frac{\Phi_i}{H_i \cdot l_e} \tag{15}$$

implying that the permeance at a given operating point is a function of the non-linear ratio B_i/H_i. This nonideality is emulated in the proposed approach by making the capacitor of the equivalent circuit (Fig. 3b) non-linear.

In this study we suggest a simple approach for modeling a controlled non-linear capacitor. This model utilizes a non-linear 'transformer' [5] with a capacitive load (Fig. 4a), where the input terminals of 'transformer' emulate a non-linear capacitor behaviour.

The capacitor value reflected to the primary C_{eq} can be evaluated as follows. From

$$C = \frac{I}{\frac{dV}{dt}} \tag{16}$$

we have

$$C_{eq} = \frac{I}{\frac{d(kV)}{dt}} = \frac{1}{k}\frac{I}{\frac{dV}{dt}} \tag{17}$$

which gives

$$C_{eq} = \frac{1}{k}C. \tag{18}$$

If C is unity then

$$C_{eq} = \frac{1}{k} \tag{19}$$

where k is the 'transformer' scale factor.

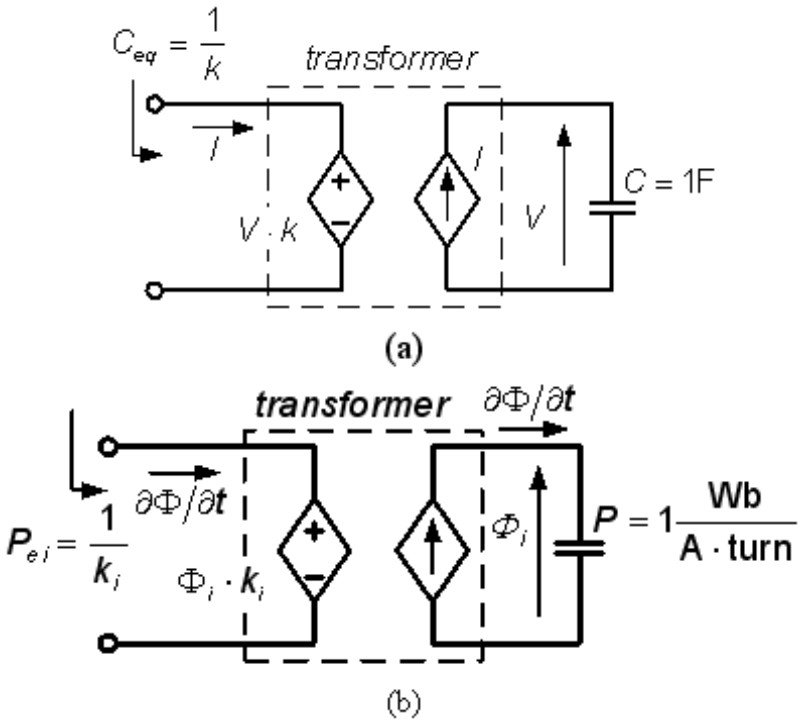

Figure 4: A variable capacitor model (a) and its application for emulating a non-linear permeance (b).

In order for the proposed model of controlled capacitor C_{eq} to emulate the behaviour of the magnetic branch permeance, the scale factor k_i (Fig. 4b) needs to be fitted to the core data:

$$P_{ei} = \frac{1}{k_i}. \tag{20}$$

From (15) and (20):

$$k_i = \frac{\{H_i\,(\Phi_i/A_e)\}\,l_e}{\Phi_i} \tag{21}$$

where the notation $\{\,H_i\,(\Phi_i/A_e)\,\}$ implies that H_i is a function of B_i and hence of (Φ_i/A_e). This relationship can be obtained from the branch's effective parameters (A_e,l_e) and the manufacturers data (in form of a table or fitted experimental equation) of the magnetic field strength H_i *vs* magnetic flux density B_i of the core.

By applying (11), (15), (21), the input transformer voltage source $\Phi_i k_i$ (Fig. 4b) can be replaced by:

$$V_C = \frac{\Phi_i}{P_{eq}} = \Phi_i k_i = \{\,H_i\,(\Phi_i/A_e)\,\}\cdot l_e = \{H_i\,(B_i)\}\cdot l_e \tag{22}$$

since $B_i = \Phi_i/A_e$.

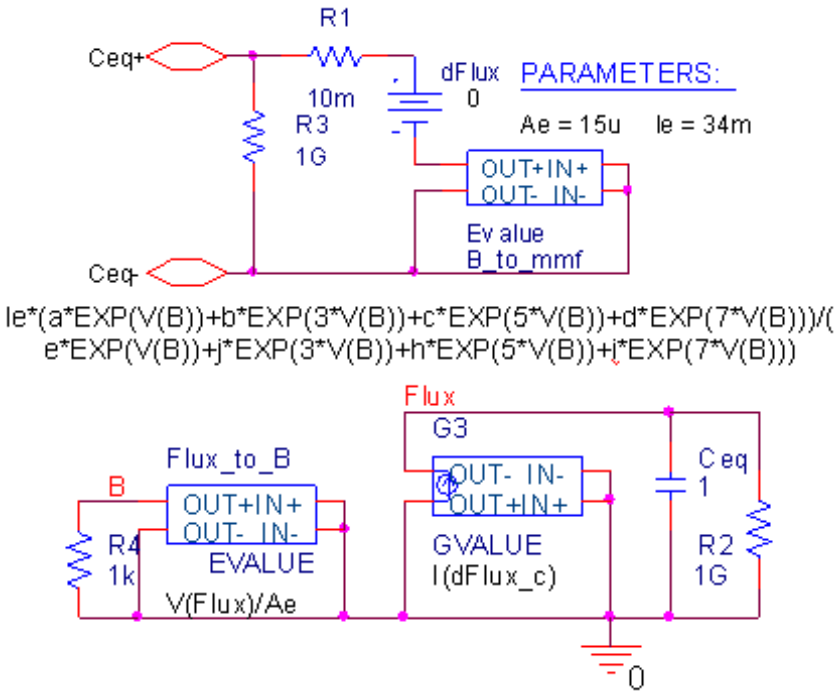

Figure 5: PSPICE (CADENCE Eval. Version 9.2) model of non-linear capacitor emulating the magnetic energy storage element. Branch parameters: $A_e = 15\,\mu m^2$ and $l_e = 34$mm. Core material: 3F3 [5].

The magnetization curve,$\{H_i(B_i)\}$, given by manufacturer [6] was fitted numerically to the expression:

$$H_i = \frac{m_1 \cdot \exp(B_i) + m_2 \cdot \exp(3B_i) + m_3 \cdot \exp(5B_i) + m_4 \cdot \exp(7B_i)}{m_5 \cdot \exp(B_i) + m_6 \cdot \exp(3B_i) + m_7 \cdot \exp(5B_i) + m_8 \cdot \exp(7B_i)} \tag{23}$$

where m_i are the fitting constants. For ferrite 3F3 [6] the fitting constants are $m_1 = 2.61$, $m_2 = -16.79$, $m_3 = 16.79$, $m_4 = -2.61$, $m_5 = -0.121$, $m_6 = 0.221$, $m_7 = 0.221$, $m_8 = -0.121$.

The same dependence $\{H_i(B_i)\}$ can also be approximated by the following expression:

$$H_i = n_1 \, Tan(n_2 \, B_i), \tag{24}$$

where n_i are the fitting constants: $n_1 = 21.83$, $n_2 = 3.56$.

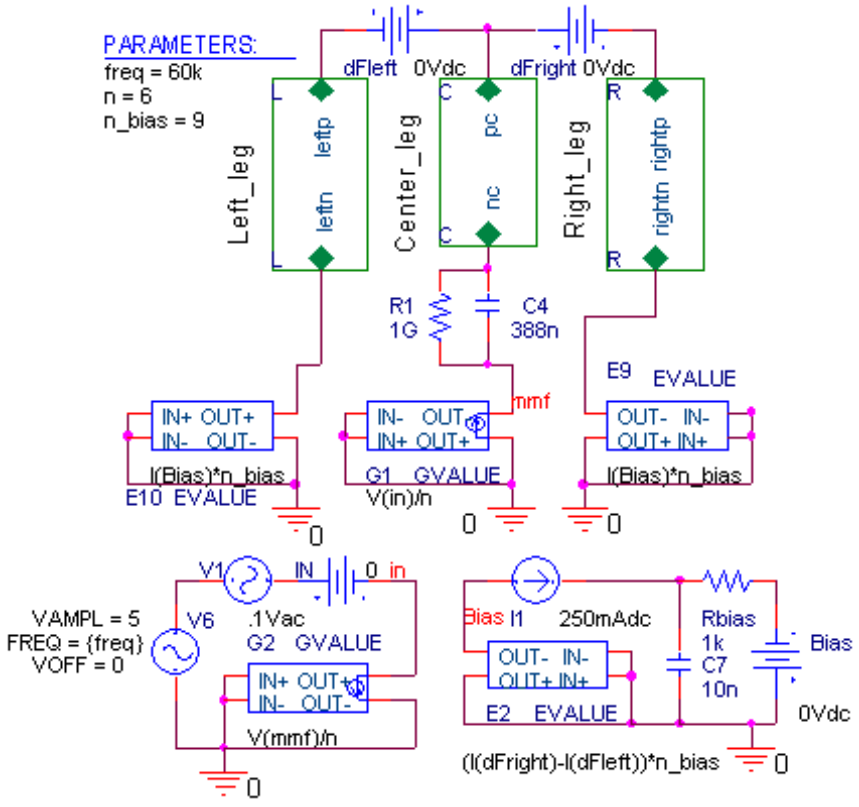

Figure 6: PSPICE model of the current-controlled inductor of Fig. 4.

Relationships (23) and (24) are identical for all the core branches provided that they are built from the same magnetic material.

To realize the controlled capacitor C_{eq} in PSPICE environment, the input 'transformer' voltage source can be partitioned into two dependent voltage sources (Fig. 5). The first one (EVALUE) samples the capacitor charge Q_{eq}, which is equal to V_{FLUX} since $P = 1\,\mathrm{Wb/A} \cdot \mathrm{turn}$. That is, V_{flux} represents Φ_i. The expression of the EVALUE V_{flux}/A_e converts Φ_i to B_i. The B_i is represented by voltage V_B. The second source (EVALUE) samples the voltage V_B and by expression (23) multiplied by l_e produces the voltage V_C (i.e. mmf).

The complementary part of the 'transformer' that feeds the input current to the capacitor P is realized by a behavioral dependent current source GVALUE.

Fig. 5 is thus a representation of a non-linear permeance of a single magnetic branch. To model a non-linear arbitrary magnetic circuit, one would need the values of effective parameters of all branches and a single H *vs* B relationship of the magnetic material (assuming that all branches are made from the same material, otherwise there would be a need for this relationship for all materials).

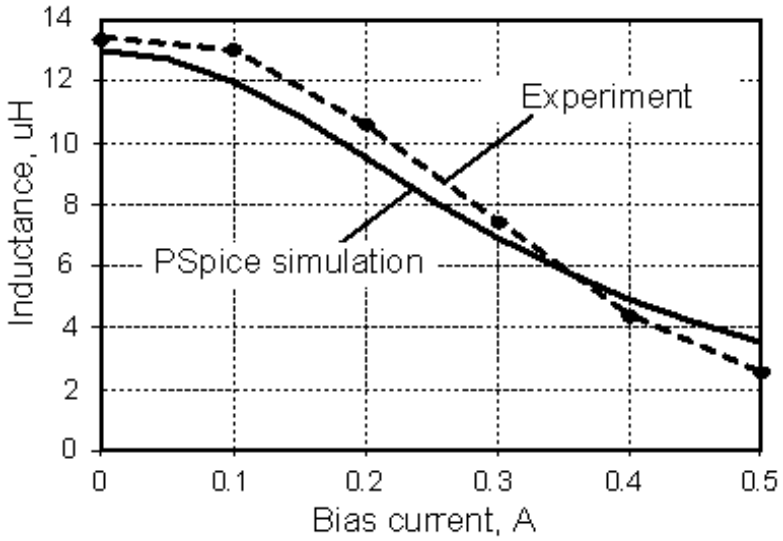

Figure 7: Simulated and measured inductance of the current–controlled inductor versus bias current I_{bias}.

To eliminate convergence problems in SPICE simulations, the model incorporates some extra resistances R1, R2 and R3. R2 provides a galvanic path to the ground, while R1 allows the connection of the node to a voltage source. It should be noted that the proposed model does not guarantee an accurate approximation of hysteretic behavior given by the core material manufacturer.

The proposed equivalent SPICE model (Fig. 6) of the current-controlled inductor includes three sub-circuits (Left_leg, Right_leg, Center_leg), which emulate the non-linear behavior of magnetic core arms. The structure of each sub-circuit is equal to the circuit depicted in Fig. 5.

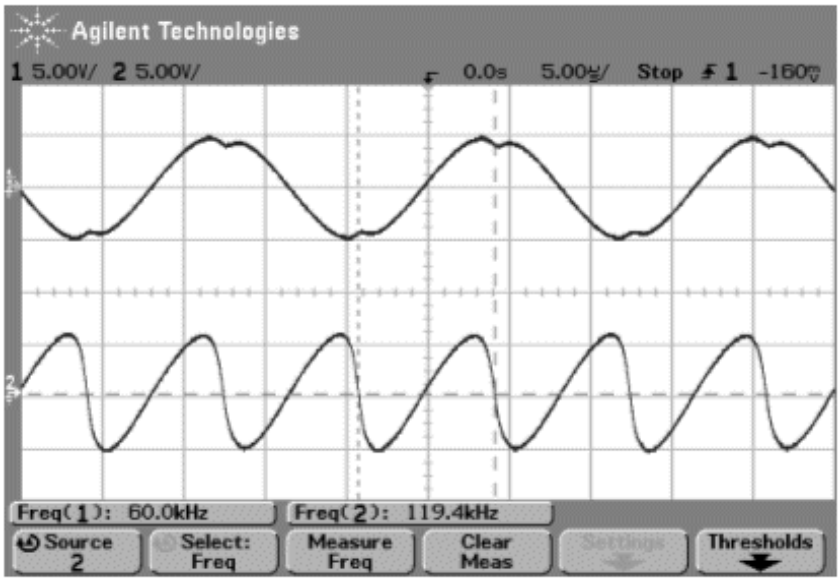

Figure 8: Experimental measurement of outer arm windings voltage V_{bias} (lower trace) and center-arm-wound-inductor input voltage V_{in} (upper trace) for I_{bias}= 0.3A. The V_{bias} frequency (120kHz) is double the frequency of input voltage V_{in} frequency (60kHz).

5 Experimental

The proposed model was verified by experimental measurements of inductance vs. bias current of a current-controlled inductor built around an EFD15. The initial center arm inductance (no bias) was $L_0 = 13\mu H$; the

numbers of turns were: $n = 6$, $n_{bias} = 9$. Close agreement was obtained between the simulated and experimental results (Fig. 7).

The effect of parasitic coupling between main and bias inductors was demonstrated by direct measurements on the experimental setup (Fig. 8). Similar results were obtained from proposed PSPICE model simulation (Fig. 9).

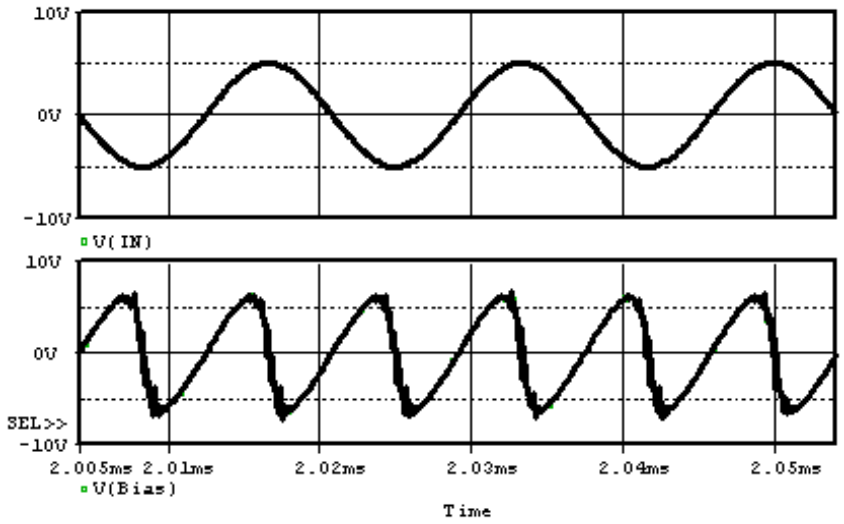

Figure 9: PSPICE simulated outer arm windings voltage V_{bias} (lower trace) for I_{bias}= 0.3A and center-arm-wound-inductor input voltage V_{in} (upper trace).

6 Discussion and conclusions

The present study is devoted to the simulation of the nonlinear behavior of the studied controlled inductor. The main advantage of the proposed modeling approach is that it makes possible to represent any given magnetization curve (excluding accurate representation of hysteretic behaviour). For close approximation of magnetization curve, the (23) and (24) can be fitted to the magnetic core manufacturer data. As a result, a good agreement between the simulations and experiments can be achieved.

The proposed modeling and simulation approach is potentially a viable tool to study the behavior of other complex integrated magnetics structures.

References

[1] D. Medini and S. Ben-Yaakov, IEEE Applied Power Electronics Conference, APEC'94, Orlando, p.219 (1994).

[2] S. Ben-Yaakov and M. Peretz, IEEE Power Electronics Specialists Conference, PESC'04, Aachen, p.61 (2004).

[3] D.C. Hamill, IEEE Applied Power Electronics Conference, APEC'94, Orlando, p.326 (1994).

[4] D. Cheng, L.P. Wong, and Y.S. Lee, IEEE Power Electronics Specialists Conference, PESC'00, New Orleans, p.320 (2000).

[5] S. Ben-Yaakov and M. Peretz, IEEE Power Electronics Society Newsletter, Fourth Quarter (2003).

[6] *Data handbook soft ferrites and accessories, Ferroxcube*, Available via the Internet link: http://www.ferroxcube.com/appl/info/HB2002.pdf